Technology Service Corporation
An Employee-Owned Small Business

6515 Main Street • Trumbull, Connecticut 06611
e-mail: info@tsc.com

Phone: (203) 268-1249 Fax: (203) 452-0260
World Wide Web: http://www.tsc.com

Ref: TSC-CT102-561

Knowledge Acquisition and Exploitation to Enhance STAP Performance

Technology Service Corporation
Paper Submission to
KASSPER Workshop
April 15, 2003

By: Allan Corbeil
Dr. Charles Morgan
Richard Pierro
Steven Jaroszewski

1.0 Introduction

Technology Service Corporation (TSC) is investigating techniques to acquire and exploit knowledge to improve the performance of Space-Time Adaptive Processing (STAP) algorithms. This work is being performed for DARPA/SPO and AFRL/SN on the Knowledge-Assisted Sensor Signal Processing and Expert Reasoning (KASSPER) program under Contract No. F30602-02-C-0034. TSC is focusing on methods to extract useful knowledge from existing databases, Ground Moving Target Indication (GMTI) radar and other sensor data including Digital Elevation Maps (DEM), Land Use/Land Cover (LU/LC) databases and Synthetic Aperture Radar (SAR) Imagery. This knowledge will be incorporated into full and reduced dimension STAP algorithms being developed by TSC and other researchers to quantitatively evaluate its benefit.

The use of DEMs and LU/LC maps in STAP could provide the following benefits. A covariance model can be developed for the clutter environment based on the terrain type (trees, desert, etc.). This covariance matrix can be employed to develop a priori filter weights that are applied to prefilter the radar returns and cancel the expected clutter interference. The residual signal can then be processed using a STAP algorithm that requires fewer degrees of freedom to cancel the remaining clutter interference. LU/LC maps can be used to subdivide the radar resolution cells by terrain type to obtain an appropriate secondary data set to better estimate the clutter covariance matrix at the target cell. LU/LC maps and DEMs can additionally delimit the surveillance area to where moving ground vehicles are likely to be present and thus eliminate false alarms. For example, heavily forested areas on steep mountain slopes far from roads can be ignored when looking for movers. Resolution cells around road networks or known discrete locations (buildings, towers) may also be excluded from the secondary data set to avoid corrupting the covariance estimate.

STAP performance can be enhanced by exploiting existing DEMs and LU/LC databases, but only if these are temporally, thematically and spatially accurate. However, these databases are sometimes grossly out of date or contain significant errors in the specified terrain type and/or boundaries between different terrain areas. The LandSat data or aerial photography upon which the LU/LC database was built may be several years old. Manual or automatically generated LU/LC maps based on any source include terrain classification errors, and small regions of unique terrain are often incorporated into larger regions of another type. DEMs such as the USGS Digital Terrain Elevation Data (DTED) contain discontinuities at cell boundaries and have widely spaced postings that miss important terrain features. TSC is developing techniques that can generate more accurate DEMs and LU/LC maps from on- or off-board sensor data.

2.0 Stereo DEM Generation

TSC is investigating two primary DEM generation techniques since DEMs are critical for mapping known scatterer locations (discretes or movers) in the object database into GMTI resolution cells for censoring. DEMs are also required to predict which cells are within shadow regions, and should not be included in estimating the clutter covariance, or involve strong terrain backscattering geometries where false alarms may occur. Ideally, the clutter covariance should be estimated using cells that are symmetric about the cell under test.

Stereo processing is based on correlating two sensor images of the same scene and determining the differential layover at each pixel. This layover is translated into a ground height for the point. The stereo geometry is illustrated in Figure 1 and calculation of the typical height accuracy which can be obtained is shown. This assumes perfect knowledge of the radar position and heading. Stereo processing can also be applied to the GMTI clutter maps that are collected

on two flight legs for a surveillance platform with different elevation look angles to the terrain. TSC is investigating the optimal GMTI radar waveform characteristics and flight path geometry for stereo DEM generation.

Another DEM generation technique being investigated is based on interferometric processing. The measured phase difference resulting from two apertures separated in elevation can be used to determine height as in interferometric SAR (IFSAR). However, apertures with horizontal spacing are generally employed for azimuth estimation in GMTI surveillance systems such as on Joint STARS. The natural pitch of aircraft in flight (or at a high angle of attack) can provide a vertical displacement of apertures on a long horizontal baseline. The resulting phase difference can then be converted into the height at each resolution cell. Robust phase unwrapping algorithms and ground control points (GCPs) are required for this DEM generation approach. Stereo processing is superior because there are no height ambiguities to be resolved and the accuracy can be controlled by simply increasing the baseline distance. However, IFSAR is potentially much more accurate, and less computationally intense.

The evaluation of stereo DEM generation techniques requires GMTI clutter maps with different flight lines. Because of the poor azimuth resolution, averaging or tomographic processing of the range-Doppler returns is also under investigation. Thus, GMTI clutter maps along an entire flight leg are desirable for stereo processing.

2.1 MTI Clutter Simulation

The data cubes being provided by ISL for the KASSPER program include only a small set of CPIs at roughly the same aircraft position and no elevation diversity is present. As a consequence, TSC is developing an in-house simulation capability that employs ERIM IFSAR-E data to model the GMTI clutter returns. The IFSAR data provides registered SAR magnitudes and terrain height with 2.5 m postings and Level 3 vertical accuracy. TSC's high fidelity radar simulation employs the SAR magnitude for the mean backscattered clutter power and computes the terrain shadowing and aspect dependence at each 3-D radar position. The effects of slant range, antenna squint angle, antenna beam gain, and range/Doppler resolution are also included, and internal clutter motion is being modeled. Data cubes of pulse by range by aperture are produced, and can additionally support the investigation of techniques that exploit SAR imagery to enhance STAP performance as described below. Figure 2 shows the radar simulation geometry with N subapertures as the aircraft moves along its flight path (motion is exaggerated). The SAR magnitude is overlayed on the DEM at the lower right. The antenna beam aimpoint and one of the contributing ground scattering points is indicated. For each beam position, a range-Doppler map is computed for each antenna aperture. Figure 3 shows various intermediate outputs of TSC's SAR-based GMTI simulation. Figure 3a shows the height map and Figure 3b indicates the resulting terrain shadowing from this particular radar look angle. The antenna gain footprint on the ground is shown in Figure 3c for this beam aimpoint. Figure 3d displays the SAR magnitude which models the clutter backscatter and Figure 3e overlays the terrain shadow onto this clutter magnitude. The effect of antenna gain is added in Figure 3f. The resulting clutter maps for two different CPI lengths are shown in Figures 4a and 4b after the effect of range and Doppler resolution is modeled. Shadow regions that appear in the high resolution output of Figure 3f show up in Figure 4 and water boundaries would also be visible, if present. The different terrain types (urban, open field) apparent in the SAR image of Figure 3d produce a unique local texture in the clutter map. This local texture, the bright spots, and shadow boundaries allow two clutter

maps to be uniquely correlated for stereo processing. TSC has developed efficient FFT-based methods of performing correlation to obtain sub-pixel registration.

2.2 Preliminary Results

A nominal racetrack flight path for a surveillance platform was defined to investigate stereo DEM accuracy. In practice, various flight geometries can be employed to achieve the required look angle diversity. Two flight legs can be flown with a significant horizontal offset at the same altitude, the same ground track can be flown at different altitudes, or crossing ground tracks can be used. Two platforms could also be flown at different altitudes to provide elevation diversity. The beam tiling to cover a Region of Interest (ROI) was also defined as shown in Figure 5. The ROI is a small square within the available IFSAR-E collection area.

Three modes of stereo operation are being studied. The first is collecting a single set of MTI dwells at the midpoint of the leg, possibly with a long CPI to enhance cross-range resolution. The second is averaging together all of the MTI dwells over an entire flight leg so as to improve the cross-range resolution. The third is to employ tomographic processing on the dwells from each separate flight leg to enhance the cross-range resolution. Ideally, the same dwell could be used for both GMTI surveillance and stereo DEM generation rather than a longer CPI. TSC is studying the effect of both dwell length and averaging on DEM accuracy. Averaging reduces the clutter scintillation and increases the effective CNR for the clutter returns of interest. The collection of clutter statistics over multiple dwells and passes for stereo processing could also benefit STAP. Clutter covariance matrices are generally estimated by assuming "spatial" egodicity. Data from multiple passes and scans could be used to estimate covariance matrices by assuming "temporal" ergodicity. The temporal clutter variation could also be used to select an optimal STAP algorithm or the required degrees of freedom.

Figure 6 presents some preliminary results of stereo DEM generation. Figure 6a displays the original input IFSAR magnitude and height data. Figure 6b shows the simulated GMTI clutter maps for two looks from different elevation angles. Figure 6c compares the estimated DEM and the Level 3 DTED ground truth for this region. A quantitative evaluation of the height accuracy is planned in the coming year.

2.3 Tomographic Processing

TSC is also investigating tomographic processing to enhance the cross-range resolution of the GMTI clutter map. In a typical surveillance system, this is much poorer than the down-range resolution. For example, in the KASSPER simulated data cube and MCARM data sets, it is a factor of 200 worse. For Joint STARS, it is roughly a factor of 20 times poorer. Averaging the MTI maps sharpens the cross-range resolution by effectively overlapping the beam footprints collected at different aspect angles. However, this is only effective for a limited range of aspect angles. Noncoherent tomography offers another means of enhancing the cross-range resolution. For each beam dwell in the ROI, a shadow graph is formed. This is known as the radon transform which sums the return power in the cross-range dimension. Since low resolution MTI and high resolution SAR maps differ mainly in their cross range resolution, line integrals along the cross range dimension of each map should contain roughly the same information. This fact motivates using tomographic processing to sharpen MTI maps along their cross range dimension. Let $f_L(x,y)$ and $f_H(x,y)$ denote, respectively, the low resolution (MTI) map and high resolution (SAR quality) magnitude maps. Also let t denote the linear variation along a line perpendicular to the look direction at aspect angle θ, given by:

$$t = x\cos\theta + y\sin\theta \tag{1}$$

The tomographic equation relating the two maps is given by:

$$f_H(x,y) = \int_0^{\pi} d\theta\, g'_\theta(t) \tag{2}$$

where $g'_\theta(t)$ denotes the filtered backprojection (FBP) of the low resolution map $f_L(x,y)$ along the line t. This FBP, in turn, can be expressed in terms of the 2-dimensional Fourier transform of $f_L(x,y)$ denoted in polar coordinates by $L(K,\theta)$, with θ being the aspect angle and K denoting spatial frequency in radians/meter. Thus, $g'_\theta(t)$is given by:

$$g'_\theta(t) = \int_{-\infty}^{\infty} dK\, |K|\, L(K,\theta) e^{-j2\pi Kt} \tag{3}$$

which is equivalent to convolution in the cross-range dimension with a high pass filter, and $g'_\theta(t)$ is the radon transform.

Figure 7 illustrates the shadow graph alongside the beam positions for the sidelooking beam geometry. The filtered back projection of these shadow graphs is then accumulated over aspect angle. This is known as the inverse radon transform and produces a sharpened GMTI clutter map which is input for stereo processing. Figure 8a compares the original SAR map used to simulate the GMTI maps with a single GMTI map in Figure 8b and averaged MTI map in Figure 8c. This average was computed over an aspect angle change of 180°. Note that no receiver noise, terrain shadowing or target fluctuation was modeled in this case. Figures 8d through 8g show the effect of increasing the tomographic integration from 120° to 180° in 20° steps. The fine features become visible at greater integration angles and the image artifacts disappear. Integration angles approaching 180° are achieved by flying an extended racetrack path to encircle the ROI. An example is illustrated in Figure 9.

3.0 SAR Exploitation

TSC is also investigating the exploitation of Interferometric SAR Imagery or SAR maps that are registered with existing USGS DTED. The geolocation of clutter discretes that are not in the Digital Feature Attribute Database (DFAD) or other database can be obtained by analyzing the SAR data using standard Fixed Target Indication (FTI) techniques. All discretes cannot be expected to be in the database since these may include newly built structures, large parked vehicles and natural objects such as rock formations that are absent from the database. Backscattering from strong distributed ground clutter that is oriented nearly normal to the radar look direction can be identified in the SAR image and from the DEM. Knowledge of these strong scattering regions can be incorporated into STAP to suppress the interference and detect nearby weak target returns. The corresponding resolution cells can be excised from the secondary data set. Adaptive detection thresholding based on SAR amplitude statistics or textural features can be applied within the corresponding GMTI radar cell. The strong clutter regions found in the SAR image can also be prefiltered from the received signals. The most promising approach may be to determine the terrain type directly from the SAR image using automatic terrain classifica-

tion techniques. Secondary data sets of the same terrain type as the target cell under test can then be chosen. This offers the potential for greater performance because the terrain classes are based on common radar signatures, which should be similar for SAR and GMTI, compared to terrain classification that is based on LandSat imagery, for example.

Knowledge derived from SAR imagery, SAR and GMTI data from the same region is required to develop and evaluate STAP techniques. TSC plans to use its SAR-based GMTI simulation for initial algorithm development. This offers perfect registration that can be degraded to study the impact of aircraft position, velocity and antenna pointing angle errors. Figure 10 shows an example of using SAR magnitude and DTED at 3-meter resolution to identify GMTI range-Doppler cells containing strong clutter. The SAR and DTED are displayed in Figures 10a and 10b, respectively. The synthesized GMTI clutter map is shown in Figure 10c with a 10-meter range and 5 Hz Doppler resolution. The SAR pixels were mapped to individual GMTI range-Doppler cells using the DTED and those cells where the maximum SAR magnitude exceeded a threshold of 36 dB are marked in black in Figure 10d. Other statistics, including the median SAR magnitude, the average and the 90^{th} percentile values, were also investigated. Resolution cells that are identified could also employ a higher CFAR threshold or ordered statistic to detect targets.

More sophisticated STAP algorithms, additional degrees of freedom or secondary data set censoring rules could also be applied to these resolution cells. TSC will investigate some of these approaches and intends to work with other researchers to find other ways to utilize knowledge derived from SAR imagery.

4.0 Discrete Scatterer Location

TSC has developed improved angle/Doppler estimation techniques to more accurately measure moving target or discrete azimuth location. This is important for excising the corresponding resolution cells from the secondary data set or for prefiltering these strong signals prior to STAP. The threshold crossings due to azimuth and Doppler sidelobes of strong discretes or movers can also be predicted more accurately to reject false alarms early in the data processing.

TSC is investigating several angle location techniques to operate with full or reduced dimension STAP, and include the Maximum Likelihood Estimator (MLE), Minimum Variance Estimator and Prony's Method. These methods are being compared with conventional beam and Doppler filter splitting. The KASSPER data cubes and ground truth provided by ISL are being employed for this analysis. In Figure 11, the detected azimuth locations obtained with PRI-staggered, post-Doppler STAP and the MLE, are shown by green diamonds. Those that associate with the target ground truth (blue crosses), provided with the KASSPER datacube, are indicated by yellow diamonds. The association window used was two range cells (30 m) by one-half of the azimuth beamwidth ($\sim 0.5^{o}$). Many of the false alarms are in the regions of strong distributed terrain clutter. In addition, a high threshold (35 dB) was set in all STAP beamformed range-Doppler cells, and those that exceeded this threshold are shown by magenta circles. Most of these are out of the target region and appear at ranges of 30-35 and 50-55 km. Those that associated with the previous false alarms (green diamonds) are displayed as cyan diamonds. In performing the reduced-dimension STAP, perfect knowledge was assumed in excising the ground truth targets and discretes from the covariance and CFAR windows. Some conclusions that can be drawn are: 1) excessive false alarms occur with a reduced-dimension STAP architecture; 2) distributed terrain knowledge can be used in the future to excise those range-Doppler cells from

the covariance and CFAR estimators; 3) strong scatterer thresholding and association with terrain reflectivity is a good indicator of false alarms.

5.0 Future Plans

TSC plans to quantify the benefits of improved DEM accuracy, knowledge derived from SAR imagery and enhanced angle estimation. The sensor, processing and platform requirements to acquire knowledge will be determined. For stereo DEM generation, the achievable DEM accuracy will be assessed as a function of baseline, GMTI dwell length, flight geometry and averaging or tomographic integration angle. For interferometric DEM generation, the achievable DEM accuracy will be evaluated as a function of aperture spacing, aircraft pitch angle and other radar and platform characteristics. Joint STARS MTI data may be available from repeated passes of the same area with an altitude change, or from a racetrack flight profile that offers sufficient elevation aspect change to demonstrate stereo DEM generation. The new AFRL SPEAR facility and measured database is one possible source of such data, or it may be available from past test flights.

TSC will also exercise its SAR-based GMTI simulation to develop techniques that exploit SAR imagery to enhance STAP performance. Various methods for determining the locations of clutter discretes and predicting strong terrain backscattering regions from SAR magnitudes and DEMs will be explored. These knowledge sources will then be incorporated into STAP algorithms and their performance will be measured in terms of receiver operating curve and other metrics.

6.0 References

A. Corbeil et al, “Environmental Knowledge Acquisition, Refinement and Exploitation”, TSC Annual Technical Report on KASSPER Program, TSC-CT102-530, Contract No. F30602-02-C-0034, October 2002.

S. Jaroszewski, “Real-Time DEM Generation from MTI Clutter Imagery”, TSC Phase 1 Final Technical Report, TSC-CT108-221, Contract No. DAAH02-00-C-R021, June 2000.

J. Bergin et al, “High-Fidelitiy Site-Specific Radar Simulation: KASSPER Data Set 2”, ISL-SCRD-TR-02-106, Contract No. F30602-02-C-0005, October 2002.

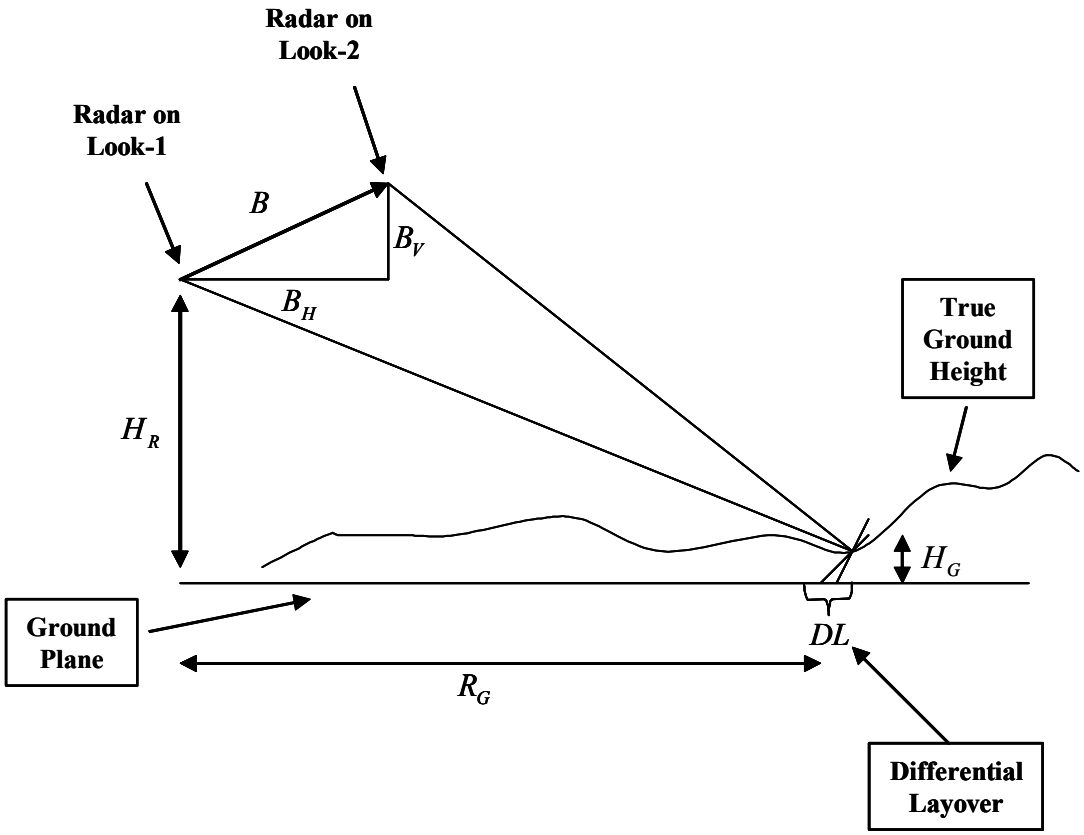

Figure 1. Stereo Geometry

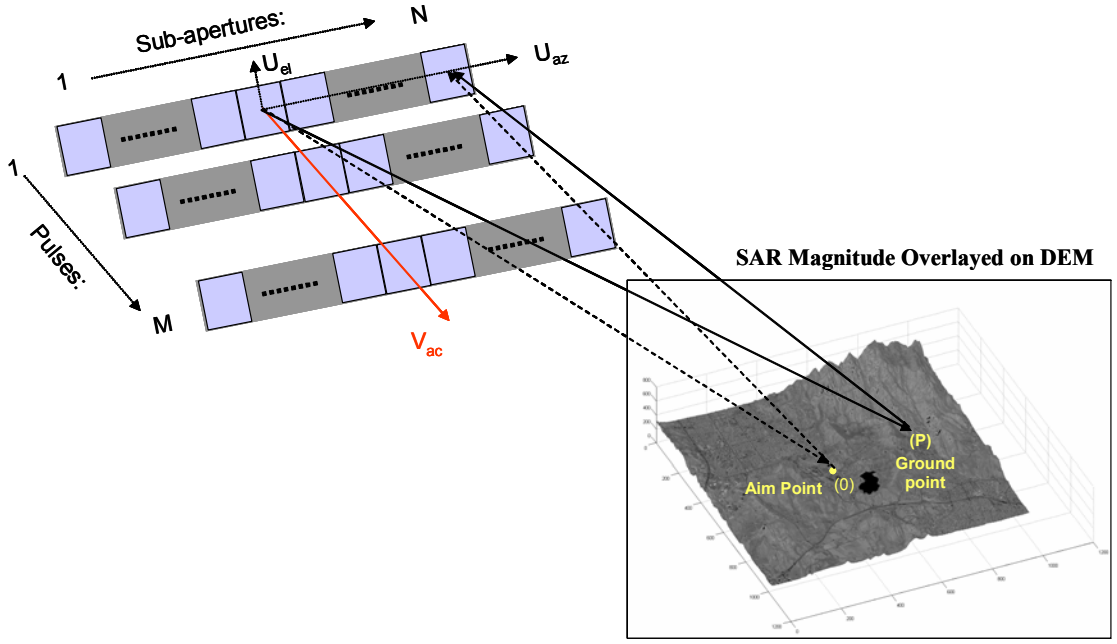

Figure 2. Multiple Aperture Simulation Geometry

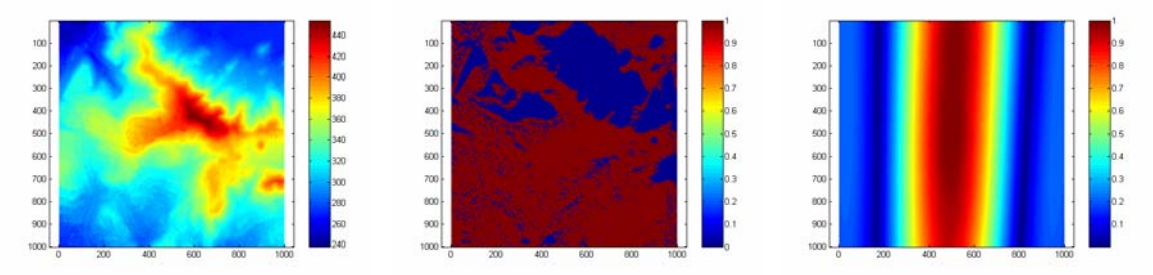

a) DTED (m) b) Shadowing (0.1) c) Antenna Gain (0-1)

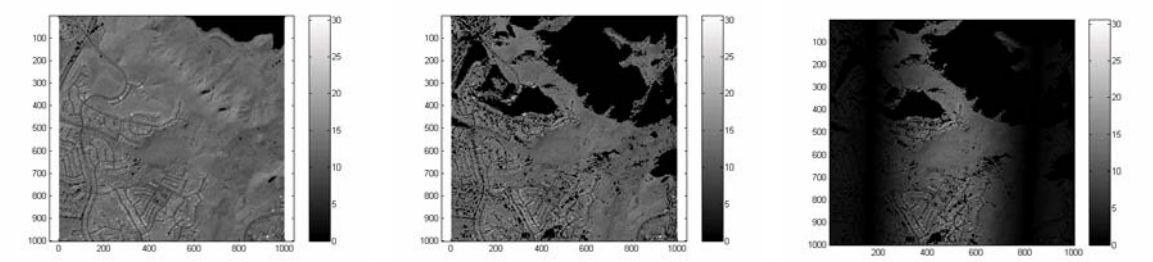

d) SAR Magnitude (db) e) Shadowed Magnitude (dB) f) Shadowed Magnitude with Antenna Gain (dB)

Figure 3. SAR-Based GMTI Simulation

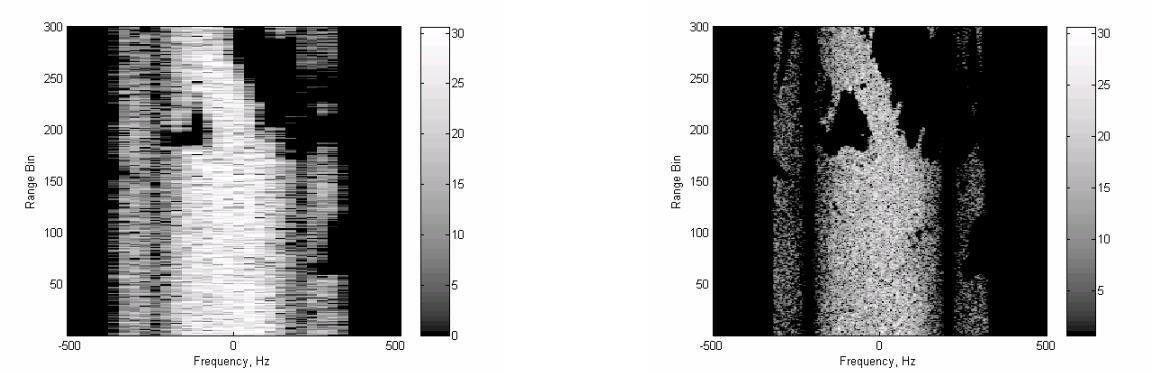

a) 32 Pulse CPI, 1 kHz PRF, Aperture #1 b) 256 Pulse CPI, 1 kHz PRF, Aperture #1

Figure 4. Range-Doppler Maps

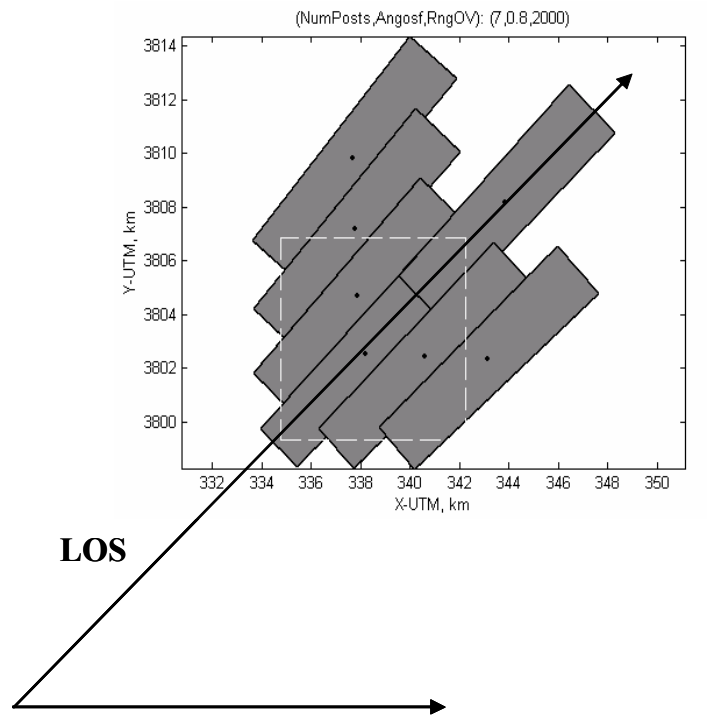

Figure 5. Beam Tiling of Region of Interest

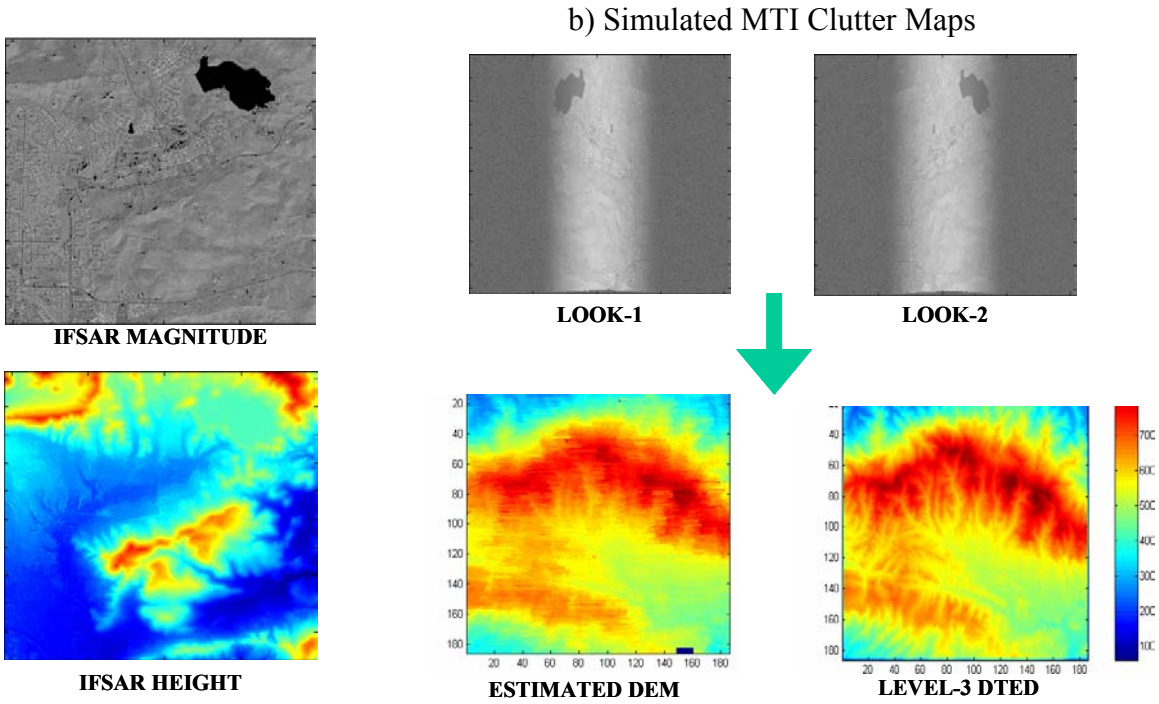

Figure 6. Preliminary Stereo DEM Generation Results

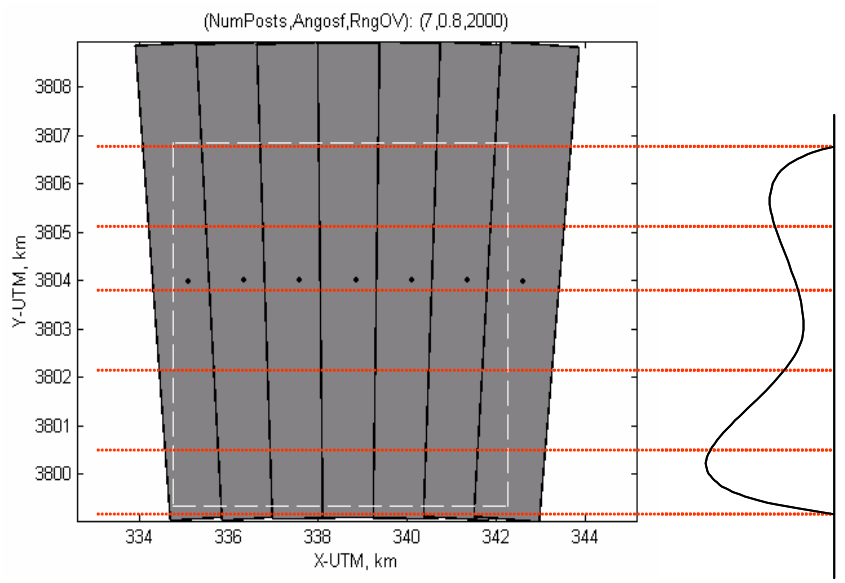

Figure 7. Illustration of Shadow Graph Formation

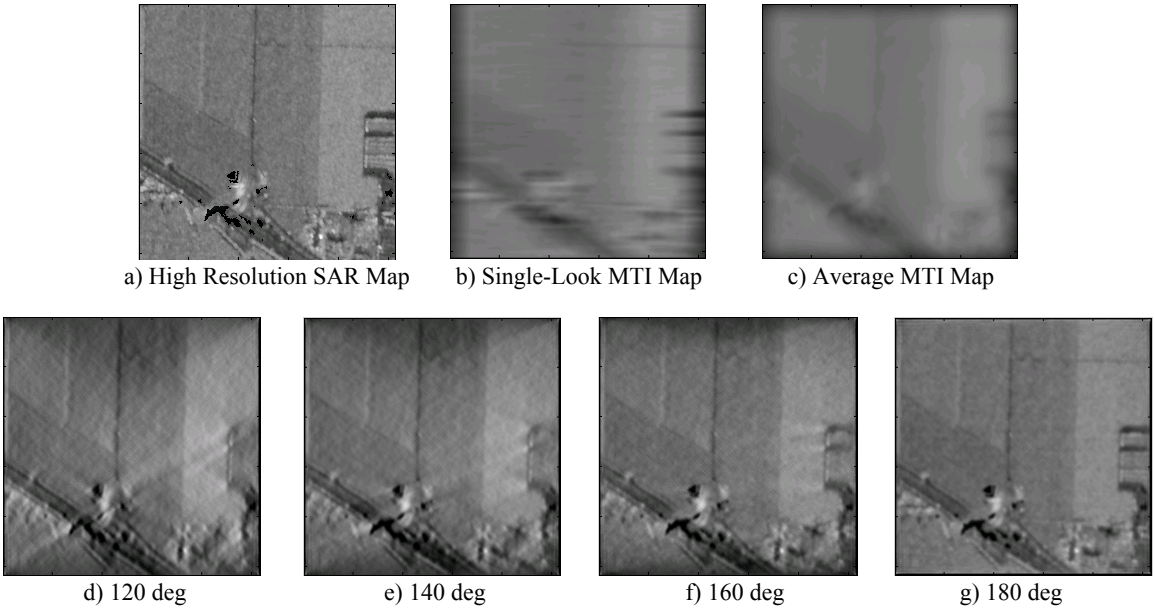

Figure 8. Examples of Noncoherent Tomographic Processing 20-to-1 Cross Range Blurring
Ideal Case: No Thermal Noise, Shadowing, or Target Fluctuation with Aspect

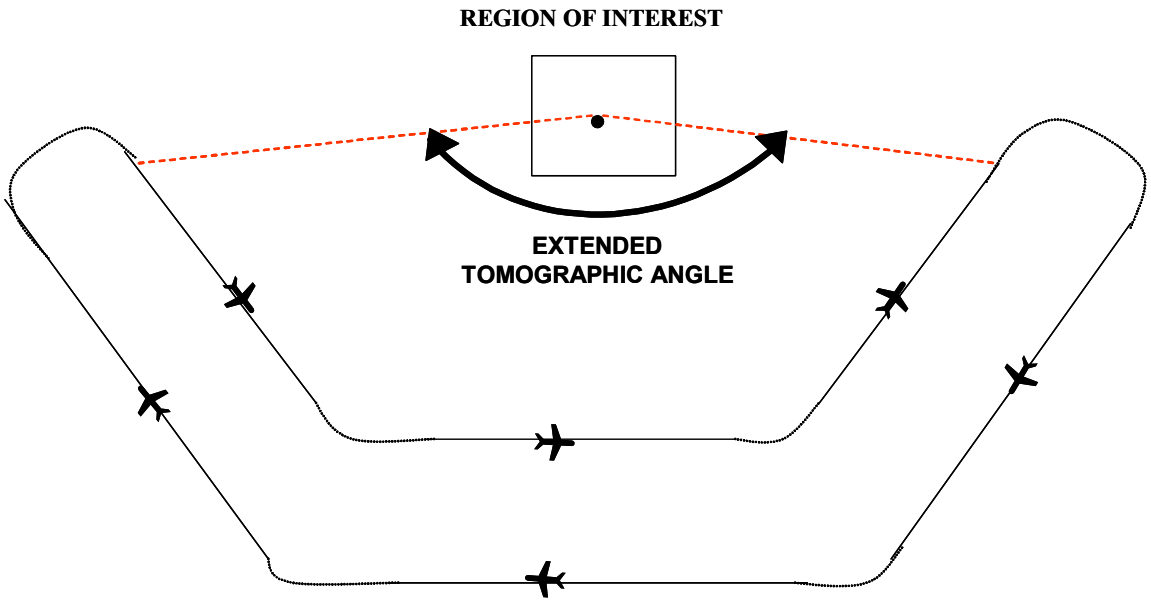

Figure 9. Extended Racetrack Flight Path

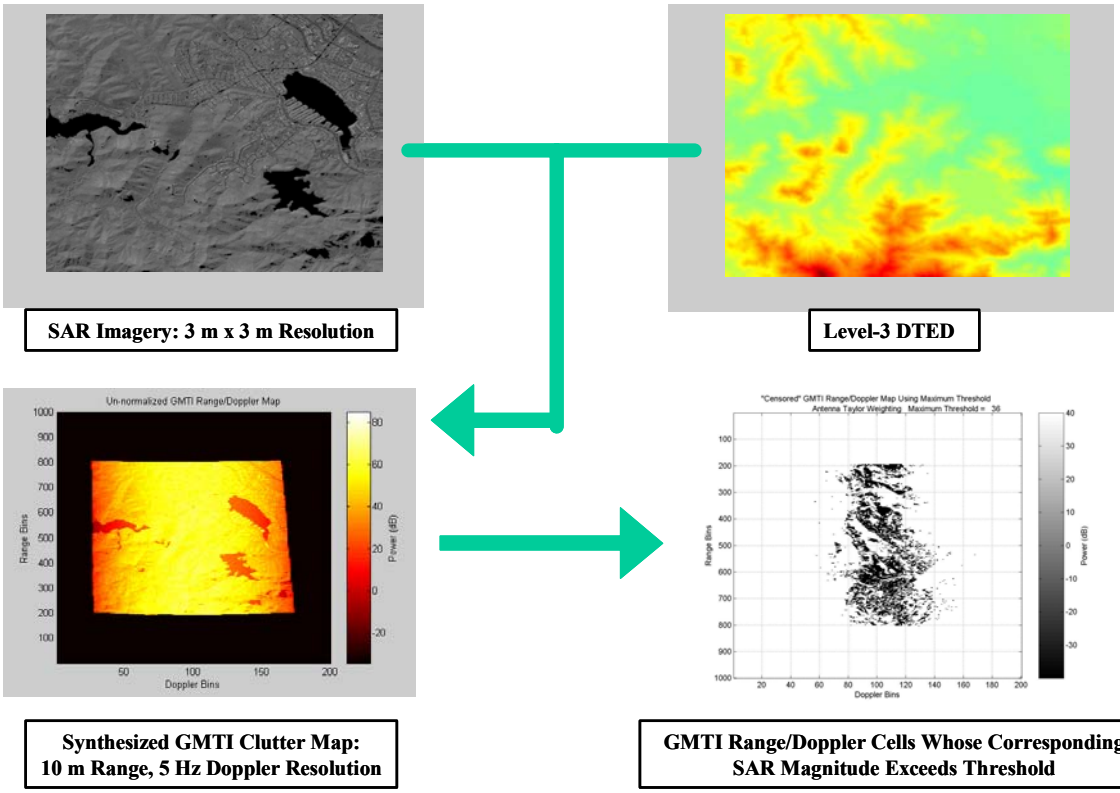

Figure 10. Example of Using SAR and DTED to Identify Strong Clutter

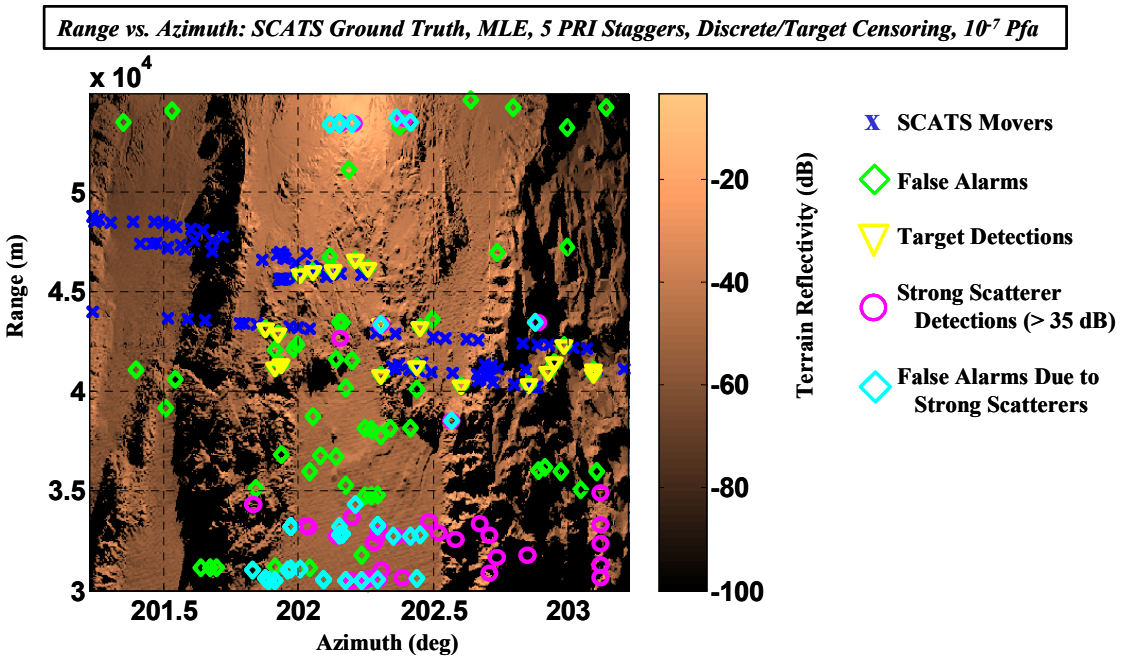

Figure 11. False Alarms and Other Data Overlayed on Terrain Cell Reflectivity